ORIGINAL RESEARCH PAPER

Multi-response Optimization of Wire EDM of Inconel 718 Using a Hybrid Entropy Weighted GRA-TOPSIS Method

P. M. Abhilash[1] · **D. Chakradhar**[1]

Abstract

The current work demonstrates a novel multi-criteria decision-making (MCDM) technique to optimize the process parameters during the wire electric discharge machining of Inconel 718. A hybrid GRA-TOPSIS algorithm using entropy weights is developed to optimize wire electric discharge machining processes parameters for maximizing the cutting speed and simultaneously minimizing the surface roughness and flatness error. Experiments were conducted according to Taguchi L_{18} orthogonal array considering pulse on time, pulse off time, servo voltage, wire feed rate, and wire electrode types as the input parameters. The weights of each responses were calculated by entropy weights method. The different alternatives were ranked using the hybrid technique, and an optimum parameter combination is found that maximizes the process outcome. The analysis of variance (ANOVA) was performed to study the relative significance of process parameters on the performance index. The results were finally validated by performing confirmation tests. The entropy weighted GRA-TOPSIS method was observed to improve the overall process performance compared to conventional TOPSIS. Microstructural analysis, morphological studies, and EDS analysis were conducted to study the surface integrity of the machined surface under optimal parameter settings.

Keywords Hybrid optimization · Wire EDM · TOPSIS · GRA · Inconel 718 · Flatness error · Entropy weights · MCDM

Abbreviations

WEDM	Wire electric discharge machining
SEM	Scanning electron microscopy
GRA	Grey relational analysis
GRC	Grey relational coefficient
TOPSIS	Technique for order of preference by similarity to ideal solution
EWM	Entropy weight method
ANOVA	Analysis of variance
MCDM	Multi-criteria decision making

Introduction

Wire electric discharge machining is a non-traditional machining process which uses repeated controlled sparks for material removal. The mechanism of material removal is by melting and vaporization of the material (Ho et al. 2004).

The process possesses several advantages over the traditional machining of hard materials due to its non-contact nature of material removal and hence offers minimal cutting forces and residual stresses. Hence, any electrically conductive material irrespective of its hardness can be machined by wire EDM process (Abhilash and Chakradhar 2021a, b, c).

In an attempt to maximize the wire EDM process performance, parametric optimization and modelling have been attempted by many researches in the past. Non-optimized parameter combinations are also reported to cause wire breakages (Abhilash and Chakradhar 2020a, b, c, 2021a). Multi-criteria decision-making (MCDM) methods are used to evaluate and rank alternatives based on multiple conflicting responses or criteria. Rajyalakshmi and Venkata Ramaiah (2013) optimized the process parameters during WEDM of Inconel 825 using Taguchi GRA method. Patel and Maniya (2015) applied analytic hierarchy process (AHP) and multi-objective optimization on the basis of ratio analysis (MOORA) method to optimize wire EDM process during the machining of EN31 alloy. Manivannan and Pradeep Kumar (2016) conducted multi-response optimization using TOPSIS method during micro-EDM process of AISI304 steel. Goswami and Kumar (2014) used utility and Taguchi's

✉ P. M. Abhilash
prj86@iitpkd.ac.in; abhilashpm184@gmail.com

1 Department of Mechanical Engineering, Indian Institute of Technology Palakkad, Kerala 678557, India

approach in multi-response optimization during wire EDM of Nimonic0 80A. Tripathy and Tripathy (2016) performed multi-objective optimization using GRA and TOPSIS methods during powder mixed EDM of H-11 die steel. Nain et al. (2017) used GRA to optimize cutting rate and surface finish during the wire EDM of Udimmet-L605. Antil et al. (2018) has performed parametric optimization of electro-chemical drilling process by considering S/N ratios of the responses. Kumar et al. (2019) optimized the process parameters during the WEDM of Ti-6Al-4 V alloy using GRA and modelled the responses using ANFIS. Antil et al. (2019) developed a multi-objective genetic algorithm to optimize electro-chemical discharge machining of SiCp/glass fiber polymer metal composites. The experiments were conducted according to Taguchi's design, and the responses considered were material removal rate and overcut. The method was reported to be effective in ensuring high MRR with a minimal overcut. Pattnaik and Sutar (2021) optimized the wire EDM process using a hybrid Taguchi neural network model. Multi-response optimization of mon traditional machining process was attempted by Das and Chakraborty (2020a, b) using a distance from mean solution method in fuzzy situation. Antil et al. (2020) have performed a GRA optimization during EDM of Ti-6Al-4 V and have reported the capability of the model to effectively optimize the parameters during electrical discharge machining to maximize productivity and surface finish.

Puhan et al. (2013) coupled PCA, fuzzy, and Taguchi methods for multi-response optimization during EDM of AlSiCp MMC. Analysis of variance revealed that pulse duration and duty cycle were the most significant parameters. Tiwary et al. (2013) used a hybrid fuzzy TOPSIS method to optimize the micro EDM process. Pradhan (2013) developed a hybrid GRA coupled principle component analysis (PCA) method to optimize the process responses during the EDM of AISI D2 tool steel. Babu Rao and Gopala Krishna (2013) performed hybrid Taguchi PCA optimization of wire EDM of ZC63/SiCp MMC. Mohanty et al. (2017) used a quantum behaved PSO (QPSO) to optimize EDM parameters during the machining of Inconel 718 super alloy. QPSO performed better in terms of computational efficiency and convergence. A hybrid grey-fuzzy logic optimization method was performed by Dewangan et al. (2015) during EDM of AISI P20 tool steel. Rao (2016) and Majumder et al. (2017) used a hybrid GRA-PCA Taguchi method for optimizing wire electric discharge machining process. Dhuria et al. (2017) developed a hybrid entropy-based GRA method to optimize the process parameters during the ultrasonic machining of Ti-6Al-4 V alloy. Mohanty et al. (2018) developed a hybrid TOPSIS-based teaching learning-based optimization (TLBO) algorithm to optimize process parameters during cryo-treated EDM of Inconel. Nain et al (2018) used a combined SVM GRA algorithm for modelling and optimization

of wire EDM of Udimet-L605. Pulse on time was observed as the most significant parameter influencing the responses. Kavimani et al. (2019) performed a hybrid Taguchi coupled GRA optimization during wire EDM of graphene – SiC-magnesium composite. Das and Chakraborty (2020a, b) performed a superiority and inferiority based MCDM method to optimize laser cutting process.

From the literature survey, it is observed that maximum efficiency for wire EDM process is often not achieved due to the improper selection of parameters. The stochastic process mechanism and involvement of various uncontrollable factors demand for an empirical study to maximize process performance. The improper selection of parameters can also result in short circuiting and wire breakages which affect productivity and part quality. Hybrid optimization techniques are attempted to better the performance of conventional decision-making methods. Inconel 718 is been used extensively for Gas turbine applications which requires high surface finish and geometric accuracy. Also, for the process to be efficient, the productivity should also be high. In this aspect, a multi-response optimization of wire EDM of Inconel 718 by considering these 3 responses are of great importance to machining fir tree–shaped turbine blades roots and disc slots. The study also analyzes the surface integrity improvement of the optimal settings over the initial settings.

Materials and Methods

Experiments were conducted according to Taguchi's L_{18} orthogonal array design. Four input parameters were considered at three levels and one parameter at two levels. The input parameters considered are pulse on time (T_{on}), pulse off time (T_{off}), servo voltage (SV), wire feed rate (WF), and wire electrode type (WT). The input parameters and corresponding levels are shown in Table 1. The ranges and levels of each parameter was selected after conducting pilot experiments and based on the information from the literature.

Table 1 Experimental settings of input parameters

Symbol	Parameters	Symbol	Level 1	Level 2	Level 3
A	Pulse on time, (μs)	T_{on}	105	110	115
B	Pulse off time, (μs)	T_{off}	40	45	50
C	Servo voltage, (V)	SV	40	45	50
D	Wire feed, (m/min)	WF	3	5	7
E	Wire type	WT	Type 1 (Zn coated brass wire)	Type 2 (Uncoated brass wire)	-

Fig. 1 a Wire electric discharge machine; **b** schematic of the process
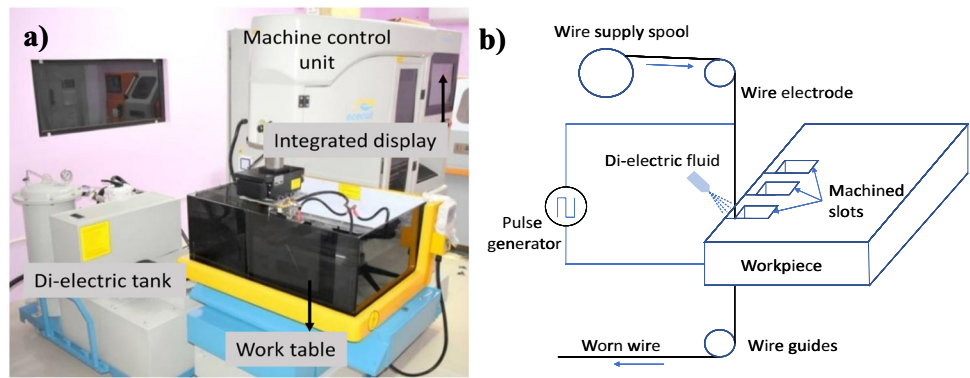
Table 2 Chemical composition of Inconel 718 (Reed 2006)

Element	Ni	Fe	Cr	Nb	C	Al	Ti	Mo
Weight (%)	Balancing	18.5	19	5.1	0.04	0.5	0.9	3

Pulse on time defines the pulse discharge energy, and it directly affects the cutting speed and roughness. Higher energy sparks creates deeper craters and makes the surface rougher. Pulse off time is utilized to clear the debris from the spark gap. Higher pulse off time results in smoother surface, but with a lesser productivity. Servo voltage determines the inter electrode gap. Low servo voltage causes spark gap bridging and thus results in rougher surface through short circuit sparks. Additionally, it creates wire vibrations which is the reason for flatness error. Wire feed rate facilitates debris flushing and is reported to cause smoother surfaces. These are the reasons for selecting these four parameters for the study. The Electronica Ecocut Wire EDM machine used for this experimental study has a default current setting for roughing operation which cannot be varied in multiple levels. This is the reason for not selecting it as a parameter.

Each experimental run was repeated thrice, and the average value is taken as response. For this study, 0.25-mm-diameter wire was used as electrode, and deionized water of 20 µS/cm conductivity was selected as dielectric fluid. Figure 1 shows the wire EDM machine used for this experimental study. An Electronica Ecocut wire EDM machine is used to conduct the experiments in this study. The machine is having 1 µm resolution on each axis. Wire electrode diameter is selected as 0.25 mm. Dielectric fluid used for this study is deionized water with ~20 µS/cm conductivity. The integrated computer displays the real-time cutting speed. Elcam software is used to generate the G and M codes for the required profile to be machined. Accurate tutor coordinate measuring machine was used to measure the form error. Surface finish was measured using Zeiss Surfcom flex 35-B surface profilometer. Zeiss GeminiSEM 300 FESEM was used for microstructural analysis. AEP Nanomap1000 non-contact surface profilometer was used to capture 3D surface morphology. The two wire electrode types chosen for

Table 3 Mechanical properties of Inconel 718 (Thakur et al. 2009)

Property	Value
Density	8.19 g/cm^3
Melting point	1260–1336 °C
Specific heat	435 J/kg K
Coefficient of thermal expansion	13 µm/m K
Thermal conductivity	11.4 W/m K
Ultimate tensile strength	1240 MPa

the study are uncoated brass wire electrode and zinc coated brass wire electrode. A rectangular profile was machined with dimensions 8 mm × 20 mm × 10 mm.

Work Material

Inconel 718 is chosen as the workpiece material for the current experimental study due to its predominant demand in aerospace and gas turbine industries. Inconel 718 is a nickel-based super alloy having superior mechanical properties especially in high temperature applications. The super alloy is largely used in the hottest sections of the gas turbines like turbine blades and disks. Apart from its high mechanical strength, the alloy is having high corrosion, fatigue, and creep resistance (Abhilash and Chakradhar 2020a, b, c). The chemical and mechanical properties of Inconel 718 are given in Tables 2 and 3.

GRA Methodology

Gray relational analysis (GRA) is based on grey system theory used to solve multi-criteria decision-making problems involving complex interrelationships between a number of alternatives and responses. GRA solves the MCDM problem

by combining coefficient values of multiple-responses to form a performance index for each alternative.

The steps involved in grey relational analysis are given below:

1. Normalization of responses is done by higher the better formula and lower the better formula as shown in Eqs. (1) and (2) respectively:

$$X_i^*(j) = \frac{X_i(j) - min[X_i(j)]}{max[X_i(j)] - min[X_i(j)]} \tag{1}$$

$$X_i^*(j) = \frac{max[X_i(j)] - X_i(j)}{max[X_i(j)] - min[X_i(j)]} \tag{2}$$

where $X_i(j)$ is the value of response parameter k.

2. Computing the grey relational coefficient (GRC) using Eqs. (3) and (4):

$$GRC_i(j) = \frac{\Delta min + \varepsilon\Delta max}{\Delta_{oi}(j) + \varepsilon\Delta max} \tag{3}$$

where

$$\Delta_{oi}(j) = X_0^*(j) - X_i^*(j) \tag{4}$$

where Δ_{max} and Δ_{min} are maximum and minimum values from normalized column. ε is weightage factor normally taken as 0.5. $\Delta_{oi}(j)$ is absolute difference between $X_o^*(j)$ and $X_i^*(j)$. $X_o^*(j)$ is the ideal normalized value for the jth response parameter considered as 1.

3. Computing the grey relational grade of each alternative which is the weighted sum of grey relational coefficients:

$$GRG_i = w_j GRC_i(j) \tag{5}$$

4. Ranking the alternatives based on their grey relational grades.

GRA-TOPSIS Methodology

GRA-TOPSIS is a hybrid MCDM method to solve complex multi-response optimization problems. Conventional TOPSIS method is said to have a few limitations including the ranking reversal (García-Cascales and Lamata 2012) and the inability to handle relative importance of the distance from the two reference points (Sanayei Amir et al. 2010). The limitations of TOPSIS can be addressed by introducing grey relational coefficient of grey relational analysis (GRA) as a replacement to the definition of geometric distance (Chen and Tzeng 2004). The hybrid GRA-TOPSIS model differs from the conventional TOPSIS in the usage of grey relational coefficient instead of geometric distance. The method differs from the conventional GRA since the algorithm finds

a compromise satisfactory solution, considering the grade relation of each alternative with respect to both the positive and negative ideal solution. The algorithm still preserves the objectivity in relation to the indication of the ups and downs of alternatives. The steps involved in hybrid GRA-TOPSIS method are as follows:

1. Formulation of decision matrix with n responses and m alternatives:

$$D_m = \begin{bmatrix} x_{11} & x_{12} & \dots & x_{1n} \\ x_{21} & x_{22} & \dots & x_{2n} \\ \vdots & \vdots & \dots & \vdots \\ x_{m1} & x_{m2} & \dots & x_{mn} \end{bmatrix} \tag{6}$$

where x_{ij} is jth response of the ith alternative.

2. Computation of normalized decision matrix by the following equation:

$$r_{ij} = \frac{x_{ij}}{\sqrt{\sum_{i=1}^m x_{ij}^2}} \; where \, j = 1,2\dots,n \tag{7}$$

3. If the weight of each response is w_j, computation of weighted normalized decision matrix, $V = [v_{ij}]$ where

$$v_{ij} = w_j r_{ij}, Given \sum_{j=1}^n w_j = 1 \tag{8}$$

4. Obtaining the positive ideal (best) and negative ideal (worst) solutions using the expressions:

$$V^+ = \left\{ \left(\sum_i^{max} v_{ij} | j \epsilon J \right), \left(\sum_i^{min} |j \int J| i = 1,2,\dots,m \right) \right\}$$
$$= v_1^+, v_2^+ v_3^+, \dots, v_n^+ \tag{9}$$

$$V^- = \left\{ \left(\sum_i^{min} v_{ij} | j \epsilon J \right), \left(\sum_i^{max} |j \int J| i = 1,2,\dots,m \right) \right\}$$
$$= v_1^-, v_2^-, v_3^-, \dots, v_n^- \tag{10}$$

5. Grey relational coefficient of each alternative with respect to "positive ideal solution" is calculated by the following equation:

$$GRC_{ij}^+ = \frac{\Delta min_j + \varepsilon\Delta max}{(v_j^+ - v_{ij}) + \varepsilon\Delta max} \tag{11}$$

Also, the grey relational coefficient of each alternative with respect to "negative ideal solution" is calculated by the following equation:

$$GRC_{ij}^- = \frac{\Delta min_j + \varepsilon\Delta max}{(v_j^- - v_{ij}) + \varepsilon\Delta max} \tag{12}$$

where $\Delta max_j = v_j^+ - v_j^-$
$\Delta min_j = v_j^- - v_j^-$
ε is the distinguished coefficient ($\varepsilon \epsilon [0, 1]$).

6. Grey relational grade is calculated as the average value of grey relational coefficients:

$$GRG_i^+ = \sum_{j=0}^{n} GRC_{ij}^+ \tag{13}$$

$$GRG_i^- = \sum_{j=0}^{n} GRC_{ij}^- \tag{14}$$

7. Calculating an alternative's relative closeness compared to the ideal solution is given by

$$P_i = \frac{GRG_i^+}{GRG_i^+ + GRG_i^-}, i = 1, 2, \ldots \ldots, m \tag{15}$$

8. Ranking the alternatives based on the descending order of P_i.

Entropy Weight Measurement Method

The entropy weight method (EWM) uses entropy to compute the amount of the information. In this method, it is considered that the difference between the attribute values is directly proportional to the information contained in it. Also, those responses which contain maximum information are given higher weights. The responses weights in the step 3 of previous section is calculated according to following steps:

1. After getting the normalized decision matrix $[r_{ij}]$, find the matrix $T = [T_{ij}]$ by the following equation:

$$T_{ij} = \frac{r_{ij}}{\sum_{i=1}^{m} r_{ij}} \tag{16}$$

2. Calculating the entropy index, e_j

$$e_j = -\frac{1}{\ln(m)} \sum_{i=1}^{m} T_{ij} \ln T_{ij} \tag{17}$$

3. Entropy weight of the j*th* response is given by w_j determined by

$$w_j = \frac{1 - e_j}{n - \sum_{j=1}^{n} e_j} \tag{18}$$

Results and Discussion

Eighteen experiments were conducted according to Taguchi L_{18} orthogonal array. The parameter combinations and responses are shown in Table 4. Cutting speed is noted directly form the display of the integrated computer of wire EDM. The cutting speed is the ratio of path length of machined profile to the total machining time. The surface roughness was measured using a contact surface

Table 4 L_{18} experimental design with responses

S. No	Input parameters					Responses		
	Wire type	Pulse on time (μs)	Pulse off time (μs)	Servo voltage (V)	Wire feed rate (m/min)	Cutting speed (mm/min)	Surface roughness (μm)	Flatness error (μm)
1	1	105	40	40	3	1.22	1.97	4.15
2	1	105	45	45	5	0.7	1.85	4.13
3	1	105	50	50	7	0.33	1.63	2.83
4	1	110	40	40	5	0.9	2.41	2.2
5	1	110	45	45	7	0.66	2.37	1.95
6	1	110	50	50	3	0.46	2.28	3.73
7	1	115	40	45	3	1.4	2.89	4.5
8	1	115	45	50	5	0.9	2.72	3.98
9	1	115	50	40	7	1.03	2.87	3.18
10	2	105	40	50	7	0.7	1.77	2.2
11	2	105	45	40	3	0.82	1.87	2.35
12	2	105	50	45	5	0.47	1.77	3.2
13	2	110	40	45	7	0.67	2.33	2.65
14	2	110	45	50	3	0.48	2.28	2.7
15	2	110	50	40	5	0.56	2.43	3.93
16	2	115	40	50	5	0.86	2.99	3.15
17	2	115	45	40	7	1.04	3.03	2.78
18	2	115	50	45	3	0.75	3.09	2.65

profilometer. The mean roughness R_a is considered the surface roughness parameter since it is most commonly used parameter in engineering applications. R_a is the arithmetic average of the height variations of the surface profile from a mean line. The parameter R_a is given by

$$R_a = \frac{1}{L} \int_0^L |Z(x)| dx \qquad (19)$$

where L is the total profile evaluation length in the x direction and $Z(x)$ represents the height function of the measured profile.

The flatness error was measured using a coordinate measuring machine (CMM). The flatness is defined in ISO 1101 as the minimum distance between two hypothetical parallel planes that can completely confine the surface under consideration as shown in Fig. 2.

The effects of variation of each input parameter on the responses are discussed next. Pulse off time is the time utilized to clear debris from spark gap. With an increase in pulse off time, non-machining time is getting increased. Therefore, the effective time utilized for machining is getting decreased, and thus overall cutting speed decreases. Also, with higher pulse off time, debris evacuation will be more effective, which causes higher proportion of ideal sparks, and thus it reduced the surface roughness. With higher pulse off time, spark gap bridging is avoided. The gap bridging causes wire oscillation which then leads to flatness error. When wire oscillations are reduced with increased pulse off time, then flatness error is also reduced.

Servo voltage determines the spark gap. When servo voltage increases, spark gap increases and vice versa. Increase in servo voltage takes the wire electrode away from work piece, and thus lesser proportion of discharge energy is passed to work piece causing reduced cutting speed. This also results in shallow craters and reduced wire vibrations, and thus surface roughness and flatness error also decrease. Increase in wire feed rate facilitates debris removal. So, due to the similar reasons explained in case of increase in pulse off time, increase in wire feed rate also decreases all the responses.
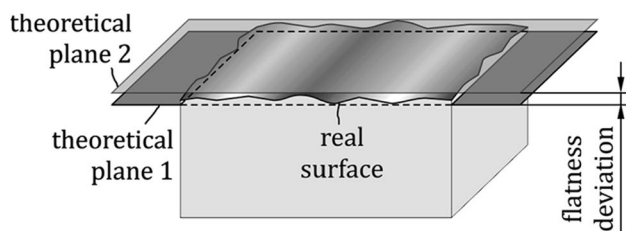

Fig. 2 Flatness deviation (Zaimovic-Uzunovic et al. 2020)

GRA-TOPSIS Computation

The normalized decision matrix is obtained by Eq. (7). The response weights were calculated by the entropy weight method using Eqs. (16), (17) and (18). The obtained entropy weights are 0.55416, 0.18083, and 0.26501 for the responses cutting speed, surface roughness, and flatness error respectively. The weighted normalized decision matrix is obtained using Eq. (8) and is given in Table 5. The positive and negative ideal solution for each response is computed by selecting the maximum or minimum value from the weighted normalized values for large the better and smaller the better responses respectively according to Eqs. (9) and (10). Positive ideal solution for cutting speed, surface roughness, and flatness error is 0.22271, 0.028828, and 0.037884 respectively. Similarly, negative ideal solution for cutting speed, surface roughness, and flatness error is 0.052495, 0.05465, and 0.087424 respectively.

The closeness coefficient values and final ranks of alternatives are given in Table 6. Experiment number 10 is ranked as the best alternative among the 18 considered followed by number 11 and number 4. The closeness coefficients of all 18 experiments are shown in Fig. 3. The maximum ranked alternative has a parameter combination of pulse on time = 105 μs, pulse off time = 40 μs, servo voltage = 50 V, and wire feed rate = 7 m/min with uncoated brass wire electrode.

Figure 4 shows the main effects plot of closeness coefficient with respect to process parameters. From the main effects plot, the optimum parameter combination that resulted in maximum closeness coefficient is $A_2B_1C_1D_1E_3$ (level 2 of wire type, level 1 of pulse on time, level 1 of pulse off time, level 1 of servo voltage, and level 3 of wire weed rate).

ANOVA for GRA-TOPSIS

The response table for mean of closeness coefficient is shown in Table 7. The relative effect of process parameters on the responses can be identified by conducting ANOVA. Table 8 shows the ANOVA results for the closeness coefficient. From the mean response table and ANOVA table, it is clear that T_{on} has the maximum effect on the responses followed by T_{off} and WF.

Confirmation Experiment

The parameter settings of $A_2B_1C_1D_1E_3$ were found optimal from the mail effects plot of the closeness coefficient using the GRA-TOPSIS method. Confirmation experiment was conducted with this parametric setting, and the results are

Table 5 Weighted normalized decision matrix

S. No	Normalized values			Weighted normalized values		
	CS*	Ra*	FE*	CS*$_w$	Ra*$_w$	FE*$_w$
1	0.350	0.193	0.304	0.194	0.035	0.081
2	0.201	0.181	0.303	0.111	0.033	0.080
3	0.095	0.159	0.207	0.052	0.029	0.055
4	0.258	0.236	0.161	0.143	0.043	0.043
5	0.189	0.232	0.143	0.105	0.042	0.038
6	0.132	0.223	0.273	0.073	0.040	0.072
7	0.402	0.283	0.330	0.223	0.051	0.087
8	0.258	0.266	0.292	0.143	0.048	0.077
9	0.296	0.281	0.233	0.164	0.051	0.062
10	0.201	0.173	0.161	0.111	0.031	0.043
11	0.235	0.183	0.172	0.130	0.033	0.046
12	0.135	0.173	0.235	0.075	0.031	0.062
13	0.192	0.228	0.194	0.107	0.041	0.051
14	0.138	0.223	0.198	0.076	0.040	0.052
15	0.161	0.238	0.288	0.089	0.043	0.076
16	0.247	0.292	0.231	0.137	0.053	0.061
17	0.299	0.296	0.204	0.165	0.054	0.054
18	0.215	0.302	0.194	0.119	0.055	0.051

Table 6 Closeness coefficient values and ranking of alternatives

S. No	Grey relational coefficients $^+$			Grey relational coefficients $^-$			GRG$^+$	GRG$^-$	Closeness coefficient, P_i	Rank
	GRC, CS$^+$	GRC, Ra$^+$	GRC, FE$^+$	GRC, CS$^-$	GRC, Ra$^-$	GRC, FE$^-$				
1	0.748	0.682	0.367	0.375	0.395	0.785	0.599	0.518	0.536	5
2	0.433	0.768	0.369	0.591	0.371	0.775	0.524	0.579	0.475	10
3	0.333	1.000	0.592	1.000	0.333	0.433	0.642	0.589	0.522	6
4	0.517	0.483	0.836	0.484	0.518	0.357	0.612	0.453	0.575	3
5	0.420	0.497	1.000	0.619	0.504	0.333	0.639	0.485	0.568	4
6	0.363	0.529	0.417	0.805	0.474	0.624	0.436	0.634	0.408	17
7	1.000	0.367	0.333	0.333	0.785	1.000	0.567	0.706	0.445	13
8	0.517	0.401	0.386	0.484	0.664	0.710	0.435	0.619	0.412	16
9	0.591	0.371	0.509	0.433	0.768	0.491	0.490	0.564	0.465	12
10	0.433	0.839	0.836	0.591	0.356	0.357	0.703	0.435	0.618	1
11	0.480	0.753	0.761	0.522	0.374	0.372	0.665	0.423	0.611	2
12	0.365	0.839	0.505	0.793	0.356	0.495	0.570	0.548	0.510	8
13	0.423	0.511	0.646	0.611	0.490	0.408	0.526	0.503	0.511	7
14	0.368	0.529	0.630	0.781	0.474	0.415	0.509	0.557	0.478	9
15	0.389	0.477	0.392	0.699	0.525	0.691	0.419	0.639	0.396	18
16	0.498	0.349	0.515	0.502	0.880	0.486	0.454	0.623	0.422	14
17	0.598	0.343	0.606	0.430	0.924	0.426	0.515	0.593	0.465	11
18	0.452	0.333	0.646	0.560	1.000	0.408	0.477	0.656	0.421	15

compared with initial settings of $A_1B_1C_1D_1E_1$ and TOPSIS settings as shown in Table 9. The obtained responses showed an increased value of cutting speed combined with better surface finish and geometric accuracy when using the hybrid algorithm. In comparison, the TOPSIS optimal condition increased the cutting rate but reduced the surface finish and geometric accuracy. The result showed that the parametric settings obtained using GRA-TOPSIS method resulted in an improved overall performance in terms of quality and productivity.
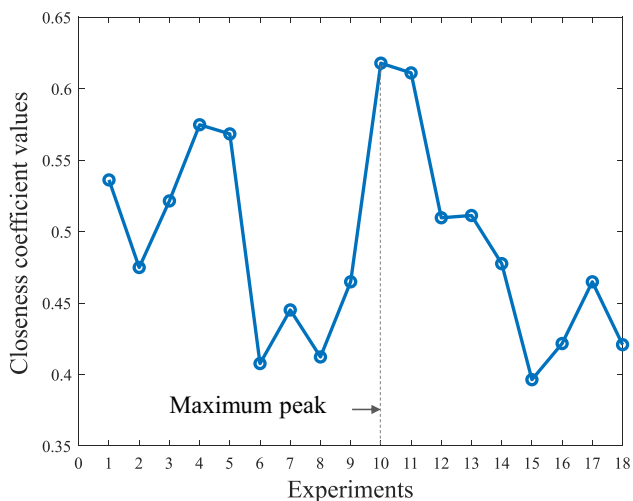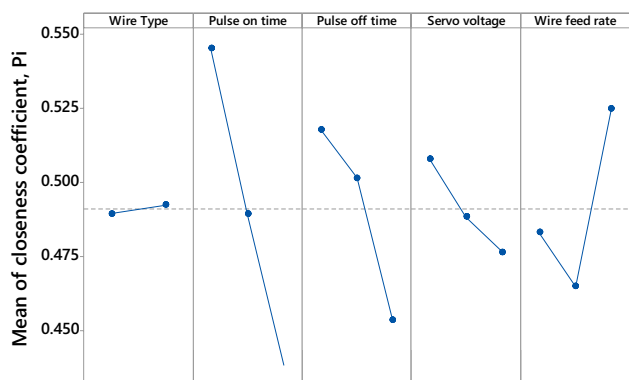
Fig. 3 Closeness coefficients of alternatives

Fig. 4 Main effects plot of closeness coefficient

Table 7 Response table for mean of closeness coefficient

| Parameter | WT | T_{on} | T_{off} | SV | WF |
	A	B	C	D	E
Level 1	0.4895	**0.5452**	**0.5178**	**0.5080**	0.4831
Level 2	**0.4924**	0.4893	0.5015	0.4884	0.4650
Level 3		0.4383	0.4535	0.4764	**0.5248**
Delta	0.0028	0.1069	0.0643	0.0316	0.0598
Rank	5	1	2	4	3

Bold values shows the highest closeness coefficient for each process parameter

Surface Morphology of Machined Surface

The machined surface morphology with initial settings ($A_1B_1C_1D_1E_1$) an optimal setting ($A_2B_1C_1D_1E_3$) is compared in this section. Figure 5a and b show the machined surface morphology captured by a non-contact 3D surface profilometer

under initial and optimal settings respectively. Higher peaks and deeper valleys are shown in Fig. 5a compared to Fig. 5b indicating a smoother surface at optimum settings.

Figure 6a and b show the microstructural images of machined surfaces captured by a FESEM under initial and optimal settings respectively. Figure 6a shows a greater number of surface defects such as micro-voids and globules in comparison to the one in Fig. 6b. The smoother surface in the latter case is a result of improved flushability due to increased wire feed rate. Also, the uncoated wire electrode used in the optimal settings is reported to result in better surface integrity.

EDS Analysis of Machined Surface

Energy-dispersive X-ray spectroscopy analysis was conducted to compare the elemental contamination of the initial parametric settings with the optimal conditions. The elements migrate from the wire electrode to the workpiece during the cutting process since the material removal happens from both workpiece and wire electrode (Abhilash and Chakradhar 2020a, b, c). Figure 7 shows the elemental analysis of machined surface under initial parameter settings (Fig. 7a) and optimal parameter settings (Fig. 7b). Since the initial parameter machines with a zinc coated electrode, weight % of zinc is more in the machined surface. However, when machined under optimal conditions, the weight percent of zinc is reduced from 4.08 to 1.91% since the wire electrode is uncoated. Thus, the optimal condition resulted in a significant reduction in zinc contamination which is recommended in machined surfaces especially in biomedical applications.

Microstructural Analysis of Wire Surface

The wire electrode considered for the initial setting is zinc-coated brass wire electrode, whereas the optimum settings recommended uncoated brass electrode. The worn wire surface after the initial and optimum settings is shown in Fig. 8a and b respectively. The wire coatings are generally a few micrometers in depth and protects the inner core from thermal shocks by "heat sink effect" (Abhilash and Chakradhar 2021a, b, c). Figure 8a shows the wire surface with numerous micro-cracks indicating the removal of outer zinc coating by meting and vaporization. The uncoated wire however does not wear by cracking but by the formation of micro-craters as evident by Fig. 8b. It is reported that uncoated wires machines surface with better geometric accuracy and surface integrity (Klocke et al. 2014). This is supported by the confirmation experiments where the optimal conditions with brass wire improved the flatness error and surface finish by 43% and 7% respectively compared to the initial conditions with coated wire.

Table 8 ANOVA table for closeness coefficient

Source	DF	Adj. SS	Adj. MS	F-value	P value	% Contribution
WT	1	0.000037	0.000037	0.01	0.909	0.04
T_{on}	2	0.034295	0.017147	6.58	0.020	41.34
T_{off}	2	0.013426	0.006713	2.58	0.137	16.18
SV	2	0.003055	0.001527	0.59	0.579	3.68
WF	2	0.01129	0.005645	2.17	0.177	13.61
Error	8	0.020854	0.002607			
Total	17	0.082956				

Table 9 Confirmation test results

Level	Initial parameter setting $A_1B_1C_1D_1E_1$	Optimal condition GRA-TOPSIS $A_2B_1C_1D_1E_3$	% Improvement
Cutting speed	1.22	1.28	4.91%
Surface roughness	1.97	1.83	7.1%
Flatness error	4.15	2.35	43.31%

Fig. 5 Surface morphology of machined surface at **a** initial parameter setting ($A_1B_1C_1D_1E_1$) and **b** optimal parameter setting ($A_2B_1C_1D_1E_3$)
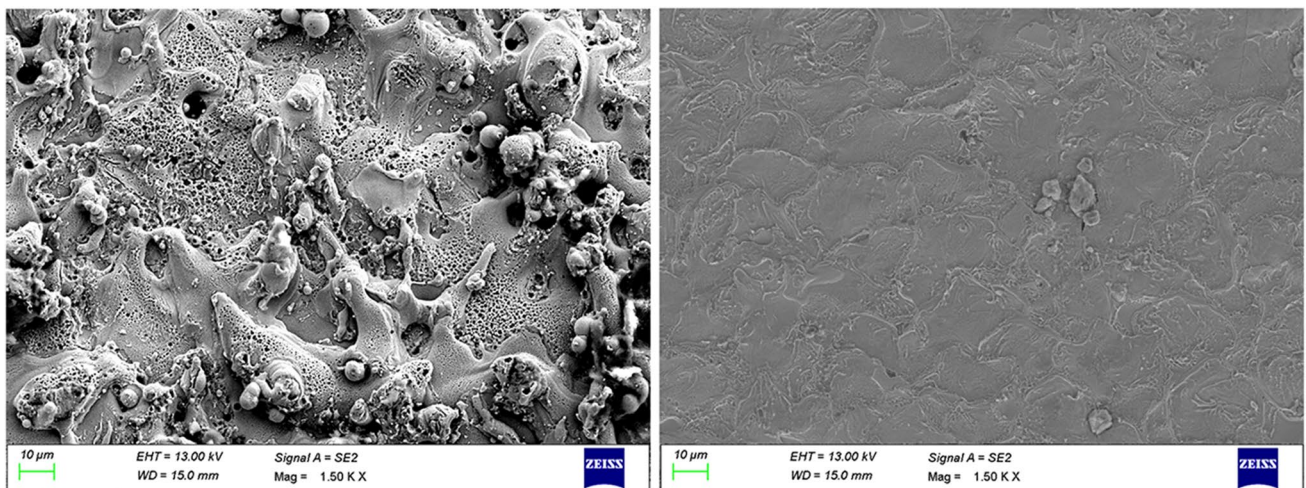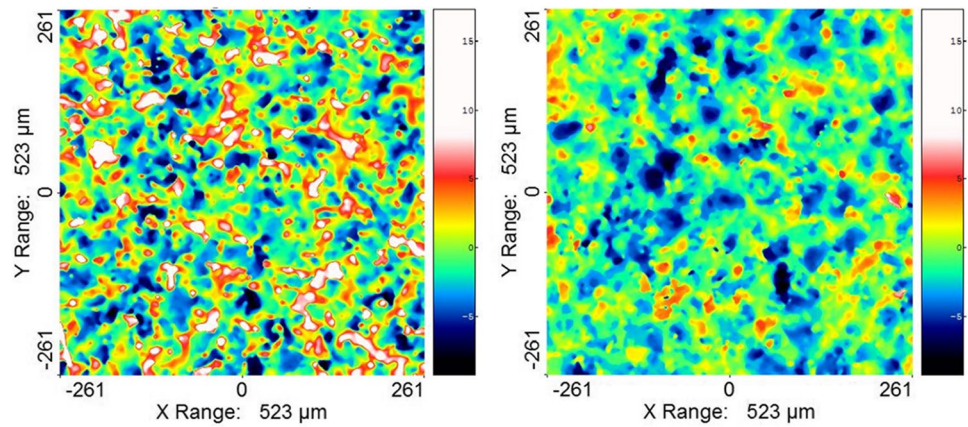

Fig. 6 SEM images of machined surface at **a** initial parameter setting ($A_1B_1C_1D_1E_1$) and **b** optimal parameter setting ($A_2B_1C_1D_1E_3$)

Fig. 7 EDS analysis of machined surfaces at **a** initial parameter setting ($A_1B_1C_1D_1E_1$) and **b** optimal parameter setting ($A_2B_1C_1D_1E_3$)

Element	Weight %
Ni	40.81
Fe	21.55
Cr	19.11
Zn	4.08
Cu	2.32

Element	Weight %
Ni	45.74
Fe	19.89
Cr	19.21
Zn	1.91
Cu	2.47
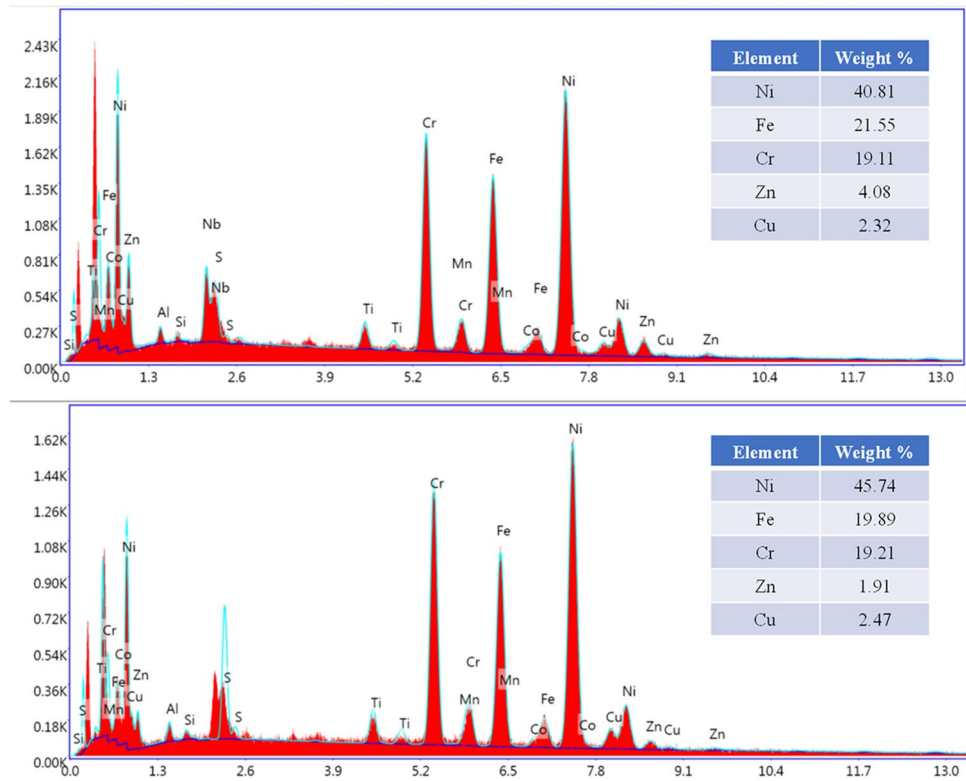
Fig. 8 SEM images of worn wire surface at **a** initial parameter setting ($A_1B_1C_1D_1E_1$) and **b** optimal parameter setting ($A_2B_1C_1D_1E_3$)
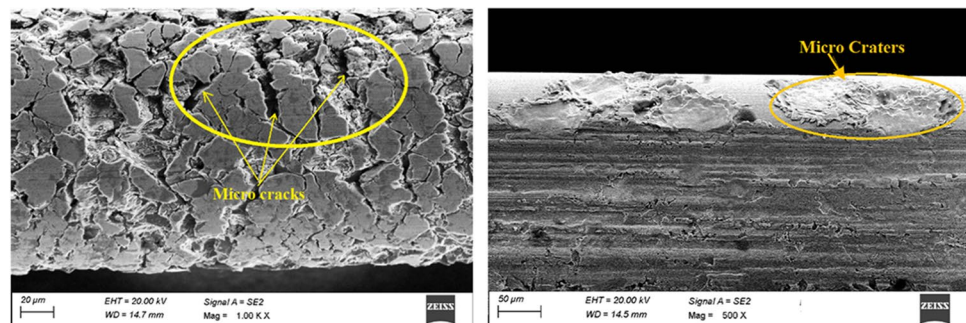
Conclusions

To maximize the efficiency of wire EDM process which involves complicated parameter interactions and a stochastic machining mechanism, a multi-objective optimization is always desirable. The paper demonstrates an entropy weighted GRA-TOPSIS algorithm to obtain optimal process parameter settings for wire EDM process during the machining of Inconel 718. Using the hybrid method, the optimal condition arrived was pulse on time at 105 µs, pulse off time at 40 µs, servo voltage at 40 V and wire feed rate at 7 m/min, with an uncoated brass wire electrode. The optimal condition cuts 5% faster with 7%

better surface finish and 43% better geometric accuracy than the initial settings. The ANOVA showed that pulse on time and off time have maximum effect on responses with 41.34% and 16.18% contribution respectively.

The emphasis of the present study is to present a novel methodology for optimal parameter selection during the wire EDM of Inconel 718. By this method, the operator can get a superior performance compared to the conventional GRA or conventional TOPSIS methods. The aim of this paper is to present the methodology and proof of concept of this method. As a future work, a comparative study can be conducted by applying the same method to multiple wire EDM machines.

Declarations

Conflict of Interest The authors declare no competing interests.

References

Abhilash PM, Chakradhar D (2020a) Surface integrity comparison of wire electric discharge machined Inconel 718 surfaces at different machining stabilities. Procedia CIRP 87:228–233. https://doi.org/10.1016/j.procir.2020.02.037

Abhilash PM, Chakradhar D (2020b) ANFIS modelling of mean gap voltage variation to predict wire breakages during wire EDM of Inconel 718. CIRP J Manuf Sci Technol 31:153–164. https://doi.org/10.1016/j.cirpj.2020.10.007

Abhilash PM, Chakradhar D (2020c) Prediction and analysis of process failures by ANN classification during wire-EDM of Inconel 718. Adv Manuf 8:519–536. https://doi.org/10.1007/s40436-020-00327-w

Abhilash PM, Chakradhar D (2021a) Failure detection and control for wire EDM process using multiple sensors. CIRP J Manuf Sci Technol 33:315–326. https://doi.org/10.1016/j.cirpj.2021.04.009

Abhilash PM, Chakradhar D (2021b) Sustainability improvement of WEDM process by analysing and classifying wire rupture using kernel-based naive Bayes classifier. J Braz Soc Mech Sci Eng 43. https://doi.org/10.1007/s40430-021-02805-z

Abhilash PM, Chakradhar D (2021c) Image processing algorithm for detection, quantification and classification of microdefects in wire electric discharge machined precision finish cut surfaces. J Micromanufacturing:1–11. https://doi.org/10.1177/25165984211015410

Antil P, Singh S, Manna A, Prakash C (2018) Electrochemical discharge drilling of polymer matrix composites. In: Sidhu S, Bains P, Zitoune R, Yazdani M (eds) Futuristic composites. Materials horizons: from nature to nanomaterials. Springer, Singapore. https://doi.org/10.1007/978-981-13-2417-8_11

Antil P, Singh S, Kumar S, Manna A, Katal N (2019) Taguchi and multi-objective genetic algorithm-based optimization during ecdm of sicp /glass fibers reinforced pmcs. Indian J Eng Mater Sci 26:211–219

Antil P, Kumar Antil S, Prakash C, Królczyk G, Pruncu C (2020) Multi-objective optimization of drilling parameters for orthopaedic implants. Meas Control 53:1902–1910. https://doi.org/10.1177/0020294020947126

Babu Rao T, Gopala Krishna A (2013) Simultaneous optimization of multiple performance characteristics in WEDM for machining ZC63/SiCp MMC. Adv Manuf 1(3):265–275. https://doi.org/10.1007/s40436-013-0029-y

Chen MF, Tzeng GH (2004) Combining grey relation and TOPSIS concepts for selecting an expatriate host country. Math Comput Model 40(13):1473–1490. https://doi.org/10.1016/j.mcm.2005.01.006

Das PP, Chakraborty S (2020a) Application of superiority and inferiority multi-criteria ranking method for parametric optimization

of laser cutting processes. Process Integr Optim Sustain 4:409–427. https://doi.org/10.1007/s41660-020-00129-4

Das PP, Chakraborty S (2020b) Multi-response optimization of hybrid machining processes using evaluation based on distance from average solution method in intuitionistic fuzzy environment. Process Integr Optim Sustain 4:481–495. https://doi.org/10.1007/s41660-020-00135-6

Dewangan S, Gangopadhyay S, Biswas CK (2015) Multi-response optimization of surface integrity characteristics of EDM process using grey-fuzzy logic-based hybrid approach. Eng Sci Technol Int J 18(3):361–368. https://doi.org/10.1016/j.jestch.2015.01.009

Dhuria GK, Singh R, Batish A (2017) Application of a hybrid Taguchi-entropy weight-based GRA method to optimize and neural network approach to predict the machining responses in ultrasonic machining of Ti–6Al–4V. J Braz Soc Mech Sci Eng 39(7):2619–2634. https://doi.org/10.1007/s40430-016-0627-2

García-Cascales MS, Lamata MT (2012) On rank reversal and TOPSIS method. Math Comput Model 56(5–6):123–132. https://doi.org/10.1016/j.mcm.2011.12.022

Goswami A, Kumar J (2014) Optimization in wire-cut EDM of nimonic-80A using Taguchi's approach and utility concept. Eng Sci Technol Int J 17(4):236–246. https://doi.org/10.1016/j.jestch.2014.07.001

Ho KH, Newman ST, Rahimifard S, Allen RD (2004) State of the art in wire electrical discharge machining (WEDM). Int J Mach Tools Manuf 44(12–13):1247–1259. https://doi.org/10.1016/j.ijmachtools.2004.04.017

Kavimani V, Soorya Prakash K, Thankachan T (2019) Multi-objective optimization in WEDM process of graphene – SiC-magnesium composite through hybrid techniques. Meas J Int Meas Confed 145:335–349. https://doi.org/10.1016/j.measurement.2019.04.076

Klocke F, Welling D, Klink A, Veselovac D, Nöthe T, Perez R (2014) Evaluation of advanced wire-EDM capabilities for the manufacture of Fir tree slots in Inconel 718. Procedia CIRP 14:430–435. https://doi.org/10.1016/j.procir.2014.03.039

Kumar Dhanabalan SS, Narayanan CS (2019) Application of ANFIS and GRA for multi-objective optimization of optimal wire-EDM parameters while machining Ti–6Al–4V alloy. SN Appl Sci 1(4):1–12. https://doi.org/10.1007/s42452-019-0195-z

Lan T-S (2009) Taguchi optimization of multi-objective CNC machining using TOPSIS. Inf Technol J 8:917–922

Majumder H, Paul TR, Dey V, Dutta P, Saha A (2017) Use of PCA-grey analysis and RSM to model cutting time and surface finish of Inconel 800 during wire electro discharge cutting. Meas J Int Meas Confed 107:19–30. https://doi.org/10.1016/j.measurement.2017.05.007

Manivannan R, Pradeep Kumar M (2016) Multi-response optimization of micro-EDM process parameters on AISI304 steel using TOPSIS. J Mech Sci Technol 30(1):137–144. https://doi.org/10.1007/s12206-015-1217-4

Mohanty CP, Mahapatra SS, Singh MR (2017) An intelligent approach to optimize the EDM process parameters using utility concept and QPSO algorithm. Eng Sci Technol Int J 20(2):552–562. https://doi.org/10.1016/j.jestch.2016.07.003

Mohanty CP, Mantra PS, Siba SM, Manas RS (2018) Optimization of cryo-treated EDM variables using TOPSIS-based TLBO algorithm. Sadhana Acad Proc Eng Sci 43(4). https://doi.org/10.1007/s12046-018-0829-7

Nain SS, Garg D, Kumar S (2017) Modeling and optimization of process variables of wire-cut electric discharge machining of super alloy Udimet-L605. Eng Sci Technol Int J 20(1):247–264. https://doi.org/10.1016/j.jestch.2016.09.023

Nain SS, Garg D, Kumar S (2018) Evaluation and analysis of cutting speed, wire wear ratio, and dimensional deviation of wire electric discharge machining of super alloy Udimet-L605 using

support vector machine and grey relational analysis. Adv Manuf 6(2):225–246. https://doi.org/10.1007/s40436-017-0192-7

Patel JD, Maniya KD (2015) Application of AHP/MOORA method to select wire cut electrical discharge machining process parameter to cut EN31 alloys steel with brasswire. Mater Today Proc 2(4–5):2496–2503. https://doi.org/10.1016/j.matpr.2015.07.193

Pattnaik S, Sutar MK (2021) Advanced Taguchi-neural network prediction model for wire electrical discharge machining process. Process Integr Optim Sustain. https://doi.org/10.1007/s41660-020-00148-1

Pradhan MK (2013) Estimating the effect of process parameters on MRR, TWR and radial overcut of EDMed AISI D2 tool steel by RSM and GRA coupled with PCA. Int J Adv Manuf Technol 68(1–4):591–605. https://doi.org/10.1007/s00170-013-4780-9

Puhan D, Mahapatra SS, Sahu J, Das L (2013) A hybrid approach for multi-response optimization of non-conventional machining on AlSiCp MMC. Meas J Int Meas Confed 46(9):3581–3592. https://doi.org/10.1016/j.measurement.2013.06.007

Rajyalakshmi G, Venkata Ramaiah P (2013) Multiple process parameter optimization of wire electrical discharge machining on Inconel 825 using Taguchi grey relational analysis. Int J Adv Manuf Technol:1249–1262. https://doi.org/10.1007/s00170-013-5081-z

Rao TB (2016) Optimizing machining parameters of wire-EDM process to cut Al7075/SiCp composites using an integrated statistical approach. Adv Manuf 4(3):202–216. https://doi.org/10.1007/s40436-016-0148-3

Reed RC (2006) The superalloys fundamentals and applications. Cambridge. https://doi.org/10.15713/ins.mmj.3

Sanayei Amir S, Mousavi F, Yazdankhah A (2010) Group decision making process for supplier selection with VIKOR under fuzzy environment. Expert Syst Appl 37(1):24–30. https://doi.org/10.1016/j.eswa.2009.04.063

Thakur DG, Ramamoorthy B, Vijayaraghavan L (2009) Study on the machinability characteristics of superalloy Inconel 718 during high speed turning. Mater Des 30(5):1718–1725. https://doi.org/10.1016/j.matdes.2008.07.011

Tripathy S, Tripathy DK (2016) Multi-attribute optimization of machining process parameters in powder mixed electro-discharge machining using TOPSIS and grey relational analysis. Eng Sci Technol Int J 19(1):62–70. https://doi.org/10.1016/j.jestch.2015.07.010

Zaimovic-Uzunovic N, Lemes S, Tomasevic D, Kacmarcik J (2020) Flatness measurement on a coordinate measuring machine. In: Karabegović I (ed) New technologies, development and application II. NT 2019 lecture notes in networks and systems, vol 76. Springer, Cham. https://doi.org/10.1007/978-3-030-18072-0_19

Publisher's Note Springer Nature remains neutral with regard to jurisdictional claims in published maps and institutional affiliations.